Investigation of Autonomous Cooperation between Industrial Cooperative Humanoid Robot and Passive Balancer

Hiroaki Hanai, Toshiki Hirogaki, Mikio Ozawa, and Eiichi Aoyama
Graduate School of Science and Engineering, Doshisha University, Kyoto, Japan
Email: h871hiroaki@gmail.com, thirogak@mail.doshisha.ac.jp, 0914ozmk@gmail.com, eaoyama@mail.doshisha.ac.jp

***Abstract*—This paper proposes a method for the autonomous decentralized coordination of an industrial cooperative robot and a passive balancer. We first compared the coordination of an assist device and a human with the coordination of an assist device and a cooperative robot. This showed that there was a difference between the cooperation with a human and that with a cooperative robot in terms of vibration during operation. We confirmed that the vibration phenomenon, which did not occur in the case of human cooperation, was observed in the case of cooperation with a cooperative robot.**

***Index Terms*—component, industrial cooperative robot, humanoid robot, passive balancer, autonomous decentralized coordination, human motion**

I. Introduction

Industrial robots have contributed significantly to productivity, quality improvement, and cost reduction at production sites [1-4]. Among industrial robots, robots that can work together with humans without safety barriers are called cooperative robots because risk assessment is conducted at the time of installation, and the likelihood of serious injury is low even if an industrial robot and a human come into contact with each other. However, failure to satisfy this requirement results in a power limit of 80 W for each axis motor [5, 6]. In recent years, the Japanese government launched a new robotics strategy aimed at advancing and developing robot technology. The goal is to make Japan the world's leading society for the use of robots. To promote the social implementation of robots, inexpensive robots that can be used in all situations are required. However, it has been pointed out that there are limits to what a typical robot can do compared to a human, and that dramatic progress should not be expected even in the medium term. Therefore, rather than relying on robots for all processes in a production line, a production line in which humans and robots coexist and cooperate is expected, and the introduction of such lines is increasing. Therefore, it is important to expand the possibilities for cooperative robots [7-10].

The payload of the cooperative industrial humanoid robot in this study was 2 kg per arm, whereas the payload of cooperative robots is generally approximately 25 kg, even if they are large. Currently, the Labor Standards Law limits heavy handling to 30 kg for women over 18 years of age. Therefore, cooperative robots are not yet able to replace humans in heavy-weight handling tasks, which is an issue that needs to be addressed to promote the active use of cooperative robots.

Here, the term "power assist" is defined as a mechanical system for assisting human work actions and "to increase the ability of a person to perform a task or action or to adapt to a situation," based on the study by Seki et al. [11]. In recent years, the research and development of human power-assist technology has been active. Its origin can be traced back to the human extender proposed by Kazerooni [12, 13]. The same paper discussed the construction of a human–machine model that included an extender controlled by a human manipulation force as an input, along with the stability of the control system. In Japan, Kosuge et al. proposed a control method that could simultaneously adjust both the amplification rate of a human force and the operability and proposed a control method that introduced the idea of virtual impedance, in which a mechanical system is supposed to have the same characteristics as a tool without knowing the environment or human characteristics [14, 15]. The effectiveness of using force feedback control and impedance control as power-assist methods has been demonstrated [16].

Most of these power-assist studies have focused on human assistance, with few involving robots in control systems. Arai et al. studied the cooperative operation of a crane and robot, but the application was limited because the entire system was controlled, rather than relying on individual operations [17]. Matsui et al. also studied the coordination between a passive balancer, an assist device, and a robot; however, this was also a system in which the passive balancer was controlled by detecting the robot's movement speed with strain gauges and was not an autonomous decentralized control system [18]. In addition to the robot and assist device, sensors and other devices are necessary to achieve coordination, and these studies did not examine the characteristics of cooperative robots that would allow humans and robots to share tools. However, tool sharing is an important issue in production lines, where robots and humans coexist. Therefore, this study proposed a method for autonomous decentralized

Manuscript received April 8, 2022; revised August 30, 2022

doi: 10.18178/ijmerr.11.12.884-890

cooperation between a power-assist device and cooperative robot without a sensor.

This paper first discusses a system identification method for common passive balancer. A force/acceleration sensor capable of wireless measurements was used for this identification. These sensors are inexpensive and exhibit the same performance as those built into smartphones. Therefore, it was assumed that system identification could be performed in the field using only a smartphone. Second, we compared the assistive coordination between a person and passive balancer with that between a robot and passive balancer. This paper shows that system identification of passive balancers can be performed using inexpensive wireless measurements. It is also of academic value in that it discusses the differences in assistive coordination between cooperative robots and humans. This paper is organized as follows: Section 2 describes the experimental equipment, Section 3 identifies the passive balancer system using wireless force/acceleration sensors, and Section 4 compares the cooperation between the cooperative robot and the passive balancer and between humans and the passive balancer.

II. Experimental Equipment

A. Collaborative Humanoid Robot Hiro

This study used the humanoid robot "Hiro" (hereafter referred to as "Hiro"), which is a cooperative humanoid robot manufactured by Kawada Industries, Ltd., for research purposes, as shown in Fig. 1. The head was equipped with a stereo camera and stereo microphone to enable multimodal control of the visual and auditory senses. The definitions of the joints, coordinates, and direction of rotation of Hiro are shown in Fig. 2. The dimensions of the robot are listed in Table I. Coordinates x_r, y_r, z_r, x_l, y_l, and z_l in Fig. 1 represent the coordinates of the robot's hand tip (subscript r represents the right hand, and l represents the left hand). The coordinate origins are x_0, y_0, and z_0 in Fig. 2. Hiro's control axes have 15 degrees of freedom (DOF) for the main body and 8 DOF for the hands (4 DOF for each hand), for a total of 23 DOF. The control method was PTP control, and the speed was based on trapezoidal acceleration/deceleration. The specifications of other robots are listed in Table II. As shown in Table II, Hiro complies with cooperative robot regulations and is not designed for heavy-load work, with a one-handed payload of 2.0 kg, including the hand.

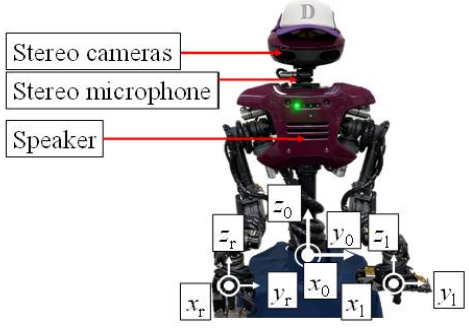

Figure 1. Humanoid robot Hiro.

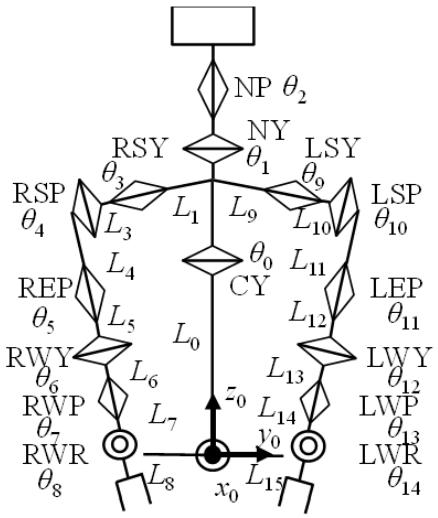

Figure 2. Composition of Hiro.

TABLE I. Hiro Dimensions (mm)

L_0	L_1	L_2, L_9	L_3, L_{10}	L_4, L_{11}	L_5, L_{12}	L_6, L_{13}	L_7, L_{14}
0	418	150	85	250	130	90	90

TABLE II. Hiro Specifications

Body weight	20 kg	
One-handed mass	0.3 kg	
Maximum payload (including hand)	2.0 kg	
Repeat positioning accuracy	0.05 mm or less	
Position control method	PTP control	
Interpolation	Angle/linear-spherical interpolation	
Speed control	Trapezoidal control	
Command minimum unit	Position	0.001 mm or less
	Angle	0.001 °

B. Passive Balancer

This study used the electric balancer "Moon Lifter," which was manufactured by the Unipulse Corporation, as shown in Fig. 3. Here, z_a is the coordinate system of the passive balancer in the vertical direction. Hereafter, this is referred to as the passive balancer. The word "passive" here means that the thrust causes acceleration and motion. A passive balancer is a device that detects the weight of a suspended object with a built-in force sensor and assists a human in its vertical transport by bearing the weight of the suspended object with a servo motor. To realize cooperative work with humans, the passive balancer is impedance-controlled, and virtual equivalent mass m_a, velocity viscosity coefficient D_0, maximum static friction force f_s, and dynamic friction force f_d ($f_s = f_d$) can be adjusted to change the operability. However, in this study, equivalent mass m_a was fixed at 15.1 kg, and the investigation focused on the viscosity and friction force. In addition, as described in section III.B, the velocity viscosity coefficient was not constant during operation but was variable and viscous, depending on the operating force. Table III summarizes the main specifications of the passive balancer.

Figure 3. Passive balancer

TABLE III. PASSIVE BALANCER SPECIFICATIONS

Dimensions	314 × 179 × 176 mm
Maximum load	30 kg
Equivalent mass m_a	15.1 kg
Velocity viscosity coefficient D_0	0–10 kg/s
Maximum static / Dynamic Friction f_s / f_d	0–N
Maximum winding speed	500 mm/s

C. Wireless Force, Acceleration, and Gyro Sensors

In this study, we used wireless force, acceleration, and gyro sensors manufactured by the PASCO Corporation, which could simultaneously measure the force and acceleration on three axes, along with the angular velocity (Fig. 4). Table IV lists the specifications of the sensors, where g represents the acceleration of gravity, which has a value of 9.8 m/s^2. The force sensor detected compressive loads as positive and tensile loads as negative. In terms of performance, it was equivalent to that used in a smartphone. Thus, it was assumed that a system could be identified in the field using a smartphone.

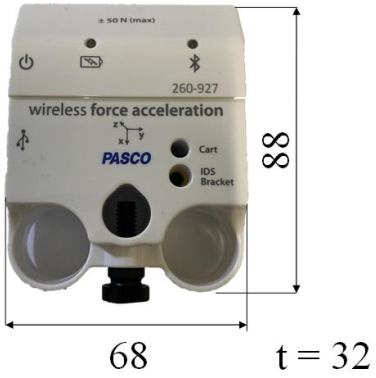

Figure 4. Wireless force acceleration sensor.

TABLE IV. SENSOR SPECIFICATIONS

Measurement range	Force	±50 N
	Acceleration	±16 g (g = 9.8 m/s^2)
Practical measurement accuracy	±1%	
Resolution	Force	0.03 N
	Acceleration	0.2 m/s^2
	Angular velocity	3 °/s
Sampling rate	200 Hz	

III. SYSTEM IDENTIFICATION OF PASSIVE BALANCER USING WIRELESS FORCE AND ACCELERATION SENSORS

A. Identification of First-Order Delay Elements in Passive Balancer

This section presents the results of preliminary experiments on passive balancer characteristics. First, the response of the passive balancer when a thrust force fin was applied was approximated by a first-order delay element to identify equivalent mass m_a [kg] and time constant T_a [s]. The mass of the weight suspended from the passive balancer was m_w [kg], and thrust f_{in} was a constant-step input. Experiments were conducted for each vertical motion. Fig. 5 shows the experimental conditions, and Table V lists the experimental conditions. This section describes the procedure for providing the step input. First, weight m_w was hung, and the system was made to memorize balanced mass m_w using the force sensor of the passive balancer. Next, weight was removed or added manually by abruptly removing or adding a weight of Δm_w from mass m_w, obtaining the detected mass $m_w \pm \Delta m_w$, and using $f_{in} = \Delta m_w g$ as the step input. The acceleration at that time was measured by the sensor described in section Ⅱ.C. Fig. 6 shows the relationship between the acceleration of the weight and time when thrust f_{in} = 2.45 N.

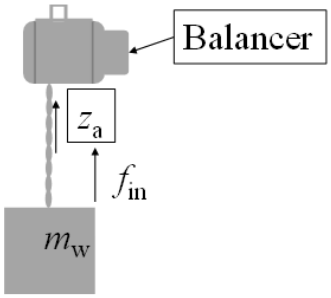

Figure 5. First-order delay element identification experiment.

TABLE Ⅴ. FIRST-ORDER DELAY ELEMENT IDENTIFICATION EXPERIMENT

Velocity viscosity coefficient D	0 kg/s
Maximum static / Dynamic Friction f_s / f_d	0 N
Suspended mass m_w	5.15 kg
Thrust f_{in}	2.45, 4.9, 7.35 N

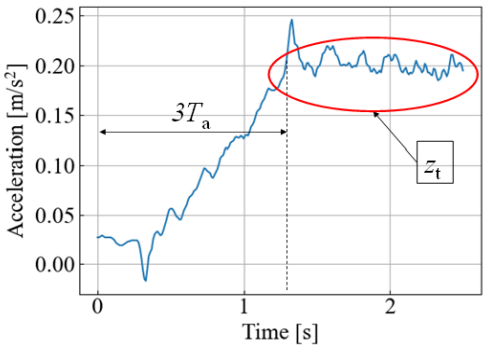

Figure 6. Step response of acceleration to thrust fin.

This figure shows how the time constant, T_a, of the first-order delay was identified by setting the time required to reach the steady-state value, z_t, to $3T_a$. The equivalent mass, m_a, described in section II.B was identified by approximating the relationship between the steady-state value of a_{zc} and thrust force f_{in} using a simple equation of motion (1). The relationship between thrust f_{in} and steady-state acceleration a_{zc} is shown in Fig. 7, and the relationship between time constant T_a and thrust f_{in} is shown in Fig. 8.

$$f_{in} = m_a a_{zc} \tag{1}$$

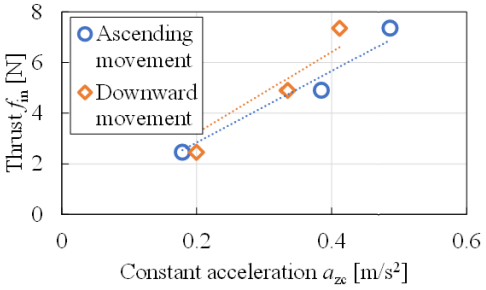

Figure 7. Identification of equivalent masses.

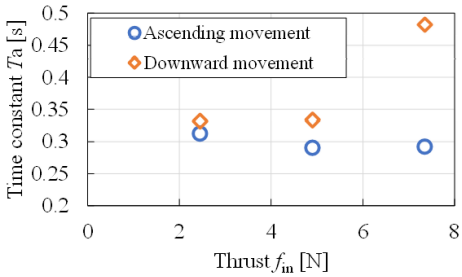

Figure 8. Identification of time constants.

From Fig. 7, it can be seen that the equivalent mass of the passive balancer, m_a = 15.1 kg, for both ascending and descending motions. Furthermore, from Fig. 8, it can be seen that time constant T_a varies slightly with the direction of motion and thrust force f_{in}, T_a = 0.33 s.

B. Identification of Operating Force-Dependent Variable Viscosity Coefficient for Passive Balancer

Next, a preliminary experiment was performed on the hypothetical velocity viscosity of the passive balancer, looking at the step response of the acceleration for a constant thrust input, as in section III. Table VI presents the experimental conditions.

TABLE VI. CONDITIONS FOR EXPERIMENT TO DETERMINE VELOCITY-VISCOSITY

Velocity-viscosity coefficient D_0	6 kg/s
Maximum static / Dynamic Friction f_s / f_d	0 N
Suspended mass m_w	5.15 kg
Thrust f_{in}	2.45 N

Fig. 9 shows the experimental results under the conditions listed in Table VI. The role of the balancer was to generate a balancing force on $m_w g$ regardless of the position and velocity of m_w. In addition, the human grasped m_w and added to or subtracted from m_w in the direction of z_a. It also assisted the human force at that time.

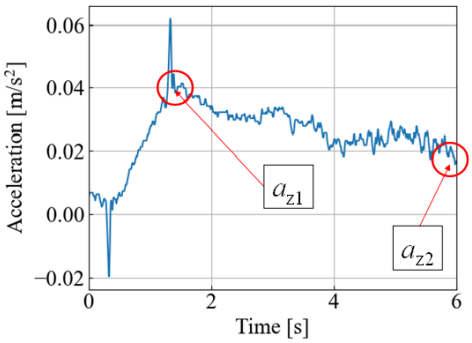

Figure 9. Step response of acceleration with velocity-viscosity coefficient added.

Fig. 9 shows that when velocity viscosity was applied, the acceleration began and then slowly decayed to a value of a_{z2}, which was half of the peak value of a_{z1}, excluding the overshoot, at approximately 6 s from the start of motion.

An operating force-dependent variable viscosity [19] was assumed. Equation (2), using the natural logarithm, was assumed for the operating force-dependent variable-viscosity coefficient, where h is the operating force, $D(h)$ is the variable-viscosity coefficient, D_0 is the viscosity coefficient at an operating force of zero, and A is a parameter representing the sensitivity of the viscosity coefficient to the operating force. The block diagram shown in Fig. 10 was simulated using MATLAB/Simulink software. Simulations were performed for different values of A. When A = 0, the rate viscosity coefficient was constant. The results of this simulation are shown in Fig. 11. The results showed that when A = 0.4, the acceleration was halved at 6 s, as in the experiment. Thus, the passive balancer is discussed below as having a variable-viscosity coefficient with sensitivity A = 0.4 to the operating force.

$$D(h) = D_0 \exp(-A|h|) \tag{2}$$

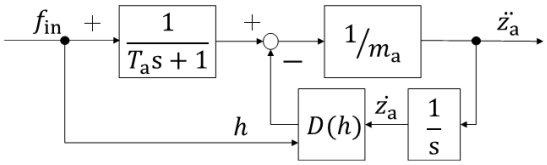

Figure 10. Block diagram including operating force dependent variable-viscosity coefficient.

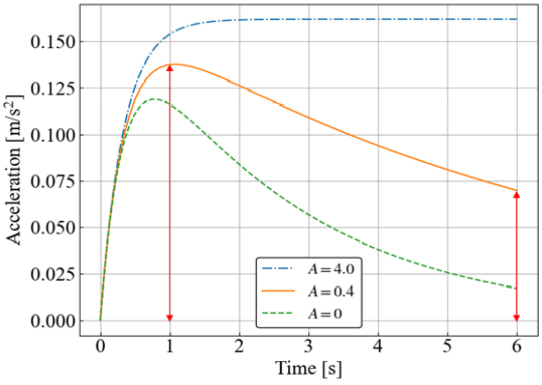

Figure 11. Effect of sensitivity of force-dependent variable viscosity.

C. Modeling of Friction in Passive Balancer

Section III.B described the operating force-dependent variable-viscosity coefficient during the assist operation. Here, the frictional force of the assist is modeled as discontinuous friction. Suppose that friction force f is added to the passive balancer system by detecting velocity v from the motor speed. The model is an object in contact with an individual surface and moves with velocity v with respect to that surface. In general, in the discontinuous friction model, frictional force f is expressed as follows, where h is the combined force of all the external forces on the object.

$$f(v,h) = \begin{cases} -h & \text{if } v = 0 \wedge |h| \le f_s \\ -\mathrm{sgn}(h) f_s & \text{if } v = 0 \wedge |h| > f_s \\ \phi(v) & \text{otherwise} \end{cases} \quad (3)$$

Here, $f_s > 0$ is the maximum static friction force, and $\phi(v)$ is any function that satisfies $\phi(v)\, v \le 0$ for all $v \neq 0$. Let $\varphi(v)$ be represented by the Coulomb friction model. The viscous force proportional to the velocity is found as follows.

$$\phi(v) = -\mathrm{sgn}(v) f_d - Dv \quad (4)$$

In general, it is difficult to use the discontinuous friction model expressed in (8) for discrete-time simulations. This is because of the definition of f at $v = 0$ (Fig. 12). In this study, we avoided this problem by defining a zero-velocity region with a finite width [20, 21]. This method can be expressed as follows. The f (v, h) values of the Karnopp model are shown in Fig. 13, where $\varepsilon = 1.0 \times 10^{-6}$. From the above, using the wireless force/acceleration sensor, the equivalent mass, time constant, and viscosity coefficient could be determined by applying thrust to the passive balancer with a step input and measuring the acceleration. The viscosity coefficient could then be identified as being dependent on the operating force.

$$f(v,h) = \begin{cases} -h & \text{if } |v| \le \varepsilon \wedge |h| \le f_s \\ -\mathrm{sgn}(h) f_s & \text{if } |v| \le \varepsilon \wedge |h| > f_s \\ \phi(v) & \text{otherwise} \end{cases} \quad (5)$$

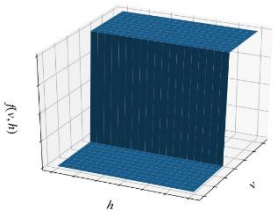

Figure 12. Coulomb friction.

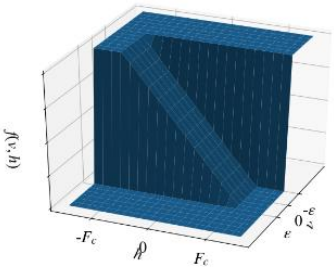

Figure 13. Karnopp friction.

IV. System Identification of Robot–Passive Balancer Systems and Discussions

In section IV, we compare the modeling and experimental results for a system in which a cooperative robot and an assist device perform cooperative actions. We focus on the differences between human-assist coordination and robot-assist coordination. Fig. 14 shows the experimental setup. The balancer and sensor fixed to the robot's paw were fixed with two bolts via a jig. Here, the vertical axis of the graph (force) measures the force generated by the robot end-effector. Fig. 15 compares the human-assist coordination and robot-assist coordination under D_0 = 3 kg/s, f_s/f_d = 0.98 N, and m_w = 5.15 kg. The robot moves 200 mm in the negative direction of z_a and the human moves the same amount. As can be seen in the figure, the human-assist coordination generates large forces at the beginning and end of the movement, but the forces during the movement are almost constant. However, in the robot-assist cooperative behavior, an oscillation component was observed during the operation. As described below, the robot comprises a positioning control system with position and velocity control loops. The input from the assist system to this control system is considered to cause motion instability. On the other hand, humans have feed-forward and feedback control systems that robots do not have, and thus, are thought to be able to perform stable movements. For example, Inaba et al. focused on and modeled the open-loop shaping characteristics of humans [22]. Typical examples of practical applications of electric power assist for humans include power steering in automobiles and the pedal motion in cars. The control focuses on the response frequency, which considers the inertia of the motor and torque fluctuation [23- 25]. Fig. 16 also shows a comparison of robots with and without assistance. The experimental conditions were similar to those shown in Fig. 14, except that the direction of the motion was positive. In this case, it can be seen that no vibrations occur without the assist but are generated during the assist coordination. Therefore, the assist coordination of cooperative robots involves vibration forces that are not present in human coordination.

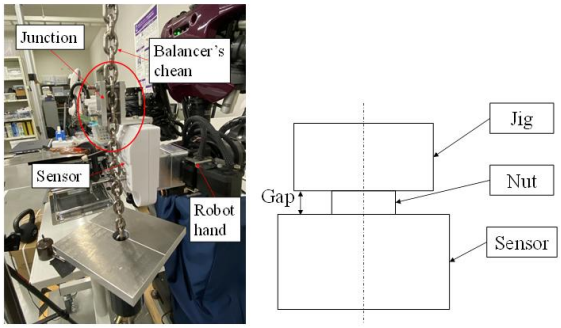

(a) Connection (b) Connection of sensor and jig

Figure 14. Sensors fixed to passive balancer and robot hand.

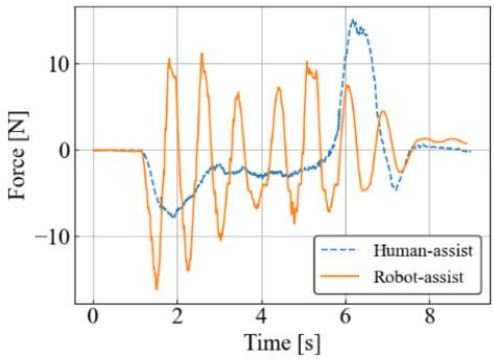

Figure 15. Comparison of human-assist coordination and robot-assist coordination.

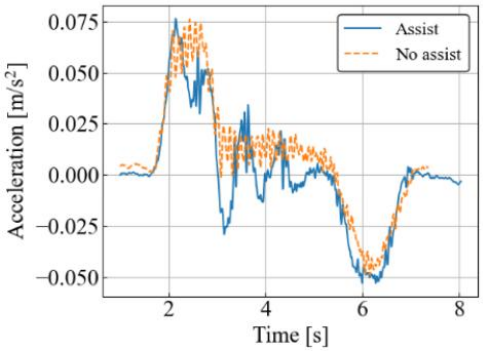

Figure 16. Comparison of robot motion with and without assistance.

V. Summary

In this paper, we proposed a method for autonomous decentralized coordination between an assist device and a cooperative robot. A method for measuring and identifying the characteristics of balancers using inexpensive wireless sensors was presented. In addition, we compared the assist-coordination of a human with that of a cooperative robot. The results are as follows.

(1) The equivalent mass, time constant and viscosity coefficient could be identified by applying thrust to the passive balancer with a step input and measuring the acceleration.
(2) The viscosity of the passive balancer depended on the operating force.
(3) It was found that vibrations that do not occur in human-assisted coordination do occur during assistive coordination with a cooperative robot.

Conflift of Interest

The authors declare no conflicts of interest associated with this manuscript.

Author Contributions

Hanai mainly conducted the research with the assistance of Ozawa. Hanai analyzed the data. Hanai wrote the paper mainly under the advice of Hirogaki. All authors had approved the final version.

References

[1] J. Arents and M. Greitans, "Smart industrial robot control trends, challenges and opportunities within manufacturing," *Applied Sciences*, vol. 12, no. 937, 2022.
[2] Q. Wu, Y. Liu, and C. Wu, "An overview of current situations of robot industry development," *ITM Web Conf.*, vol. 17, 03019, 2018.
[3] F. Kanehiro, "Cooperative works by a human and a humanoid robot," in *Proc. 2003 IEEE International Conference on Robotics and Automation*, pp. 2985-2991, 2003.
[4] Z. Ruishu, Z. Chang, and Z. Weigang, "The status and development of industrial robots," in *Proc. IOP Conference Series: Materials Science and Engineering*, vol. 423, 012051, 2018.
[5] R. W. Ghrist and D. E. Koditschek, "Safe cooperative robot dynamics on graphs," *SIAM Journal on Control and Optimization*, vol. 40, iss. 5, pp. 65–70, 2022.
[6] N. Pedrocchi, F. Vicentini, M. Matteo, and L. M. Tosatti, "Safe human-robot cooperation in an industrial environment," *International Journal of Advanced Robotic Systems*, vol. 10, 27, 2017.
[7] E. Tuci, M. H. M. Alkilabi, and O. Akanyeti, "Cooperative object transport in multi-robot systems: A review of the state-of-the-art," *Front. Robot. AI*, 2018.
[8] M. H. M. Alkilabi, A. Narayan, and E. Tuci, "Cooperative object transport with a swarm of e-puck robots: robustness and scalability of evolved collective strategies," *Swarm Intell*., vol. 11, pp.185-209, 2017.
[9] A. Ghorbanpour and H. Richter, "An overview of energy-optimal impedance control of cooperative robot manipulators," arXiv 2021 : arXiv : 2106.07491.
[10] C. R. Guerrero, J. C. F. Marinero, J. P. Turiel, and V. Munoz, "Using "human state aware" robots to enhance physical human–robot interaction in a cooperative scenario," *Computer Methods and Programs in Biomedicine*, vol. 112, iss. 2, pp. 250–259, 2013.
[11] H. Seki and Y. Hori, "Control of sensorless power assist robot using variable impedance," *National Convention Record I.E.E. Japan, Industry Applications Society*, vol. 1, pp. 601–604, 2001 (in Japanese).
[12] H. Kazerooni, "Extender: A case study for human-robot interaction via transfer of power and information signals," in *Proc. IEEE Int. Workshop Rob. Hum. Commun.*, Tokyo, pp. 10–20, 1993.
[13] H. Kazerooni, J. Guo, "Human extenders," *Journal of Dynamic Systems, Measurement, and Control*, vol. 115, pp. 281–290, June 1993.
[14] K. Kosuge, K. Furuta, and T. Yokoyama, "Virtual internal model following control system: Application to mechanical impedance control," *Trans. Soc. Instrum. Contr. Eng.*, vol. 24, no. 1, pp. 55–62, 1988 (in Japanese).
[15] S. Lee and Y. Yamada, "Strategy on safety function implementation: case studyinvolving risk assessment and functional safety analysisfor a power assist system," *Advanced Robotics*, vol. 24, pp. 1791–1811, 2010.
[16] Y. Hayashibara, Y. Sonoda, T. Takubo, H. Arai, and K. Tanie, "Assist system for carrying a long object with a human-analysis of a human cooperative behavior in the vertical direction," *IEEE*, 1999.
[17] T. Arai and H. Osumi, "Heavy work handling by the cooperative control of a crane and a robot," *J. Jpn. Soc. Precis. Eng*., vol. 57, no. 3, pp. 467–472, 1991 (in Japanese).
[18] T. Matsui, S. Amiya, S. Kobashi, K. Kikuchi, Y. Tokoro, and T. Niinomi, "Applications of robots to assembly lines," *Hitachi Rev*., vol. 64, no. 12, pp. 893–898, 1982 (in Japanese).

[19] N. Takesue, H. Murayama, K. Fujiwara, K. Matsumoto, H. Konosu, and H. Fujimoto, "Kinesthetic assistance for improving task performance: The case of window installation assist," *Int. J. Automation Technology*, vol. 3, no. 6, pp. 663–670, 2009.
[20] D. Karnopp, "Computer simulation of stick-slip friction in mechanical dynamic systems," *J. Dyn. Sys. Meas. Contr.*, vol. 107, pp. 100–103, 1990.
[21] R. A. Romano and C. Garcia, "Karnopp friction model identification for a real control valve," *IFAC Proceedings Volumes*, vol. 41, no. 2, pp. 14906–14911, 2008.
[22] T. Inaba and Y. Matsuo, "Loop-shaping characteristics of a human operator in manual control systems and new design method of compensators considering maneuverability," *Jpn. J. Ergon*., vol. 33, no. 3, pp. 131–140, 1997 (in Japanese).
[23] J. Song, K. Boo, H. S. Kim, J. Lee, and S. Hong, "Model development and control methodology of a new electric power steering system," in *Proc. Int. Mech. Eng.*, vol. 218, Part D : J. Automobile Engineering, pp. 967–975, 2004.
[24] H. Chen, Y. Yang, and R. Zhang, "Study on electric power steering system based on ADAMS," *Procedia Engineering*, vol. 15, pp. 474–478, 2011.
[25] N. Nazaruddein, F. Zainnuri, R. Siregar, G. Heryana, M. Adhitya and D. A. Sumarsono, "Electric power steering: an overview of dynamics equation and how it's developed for large vehicle," *IOP Conference Series: Materials Science and Engineering*, vol. 673, 012112, 2019.

Hiroaki Hanai is PhD student of faculty of science and engineering Doshisha Univrsity in Kyoto, Japan. He received his B.S. and M.S. degrees in mechanical engineering from Doshisha University in Kyoto, Japan in 2020 and 2022. His major is manufacturing and automation technology.

Mikio Ozawa is Master student t of faculty of science and engineering Doshisha Univrsity in Kyoto, Japan. He received his B.S. degrees in mechanical engineering from Doshisha University in Kyoto, Japan in 2022. His major is manufacturing and automation technology.

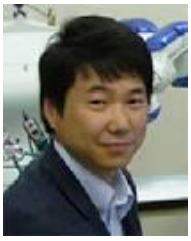

Toshiki Hirogaki is a professor of faculty of science and engineering Doshisha Univrsity in Kyoto, Japan. He received his B.S., M.S. and Ph.D. degrees in mechanical engineering from Doshisha University in Kyoto, Japan in 1988, 1990 and 1994. His major is manufacturing and automation technology.

Eiichi Aoyama is a professor of faculty of science and engineering Doshisha Univrsity in Kyoto, Japan. He received his B.S., M.S. and Ph.D. degrees in mechanical engineering from Doshisha University in Kyoto, Japan in 1976, 1978. His major is manufacturing and automation technology.